

Electroanalysis of Trace Amount Hg^{2+} Ion in Water Samples Using Sensor $\text{Co}_3\text{O}_4\text{-CeO}_2\text{-ZnO/CPE}$ and Square Wave Anodic Stripping Voltammetry (SWASV) Method

Shahnaz Davoudi*

* Department of Chemistry Omidyeh Branch, Islamic Azad University, Omidyeh, Iran

Received January 2023; Accepted February 2023

ABSTRACT

This study describes the construction of a new electrochemical sensor and applies for determination of Hg^{2+} ion. This sensor was prepared using a new nanocomposite base on ($\text{Co}_3\text{O}_4\text{-CeO}_2\text{-ZnO}$). Although the other methods (gas or liquid chromatographic, electrophoresis, flow injection) for measuring Hg^{2+} ion has advantages such as excellent accuracy and reproducibility, it has limitations such as long-time measure, high equipment cost. In this study, for determination Hg^{2+} ion we used a from sensor $\text{Co}_3\text{O}_4\text{-CeO}_2\text{-ZnO/CPE}$ and voltammetric method. The calibration curve was linear in the range of (0.03 to 35.0 μgL^{-1}). The standard deviation of less than (3%), and detection limits (3S/m) of the method (0.09 nM) for Hg^{2+} ion were obtained for the proposed electrochemical sensor by $\text{Co}_3\text{O}_4\text{-CeO}_2\text{-ZnO/CPE}$ with (95%) confidence evaluated. Finally, $\text{Co}_3\text{O}_4\text{-CeO}_2\text{-ZnO/CPE}$ has been successfully applied for the determination of Hg^{2+} ion in water samples. The method introduced to measure Hg^{2+} ion in water samples was used and can be used for other samples.

Keywords: Hg^{2+} ion; Modified electrode; Electrochemical sensor; Voltammetric method

1. INTRODUCTION

Larger among pollutants have been released into water, soil, and air environments over the past several decades. Among these pollutant heavy metals have long been recognized as a major pollutant of the environmental [1]. Wastewaters are contaminated from discharges of industrial and domestic in general different types of heavy metals like cobalt, nickel, cadmium, cuprum, chromium, lead, and zinc. These metals are among the most hazardous chemicals used

in chemical-intensive industries. The absorption of heavy metals by living organisms is due to their excessive solubility in aquatic mediums. Ingestion of large amounts of heavy metals and their accumulation in the body if they enter the food chain can cause serious health disorders [2,3].

The heavy metal ions are not biodegradable, so these ions remain in the ecological systems and food chain indefinitely. Among heavy metal ions,

*Corresponding author: sdavoudi632@gmail.com

mercury Hg^{2+} ion are well-known as toxic pollutants in the environments and ecosystems [4]. The maximum contaminant limit (MPCL) is $0.2 \mu\text{g L}^{-1}$, even low level of Hg^{2+} ion to cancer, nervous disease, kidney damage, reproductive toxicity, birth defects and skin rash [5]. Owing to the wide usage of Hg^{2+} ion, these are some of the causes of worldwide environmental pollution. Concern over the distinct toxicity of mercury has stimulated explorations aimed at developing price-favorable, fast, and facile methods to monitor mercury in biological, industrial and food samples [6]. According the stated reasons, a simple and rapid detection of Hg^{2+} ion is important in different types of real samples. Therefore, the detection of Hg^{2+} in water environment is of great significance for the protection of human health. To meet the need of Hg^{2+} sensing, traditional analytical methods, ion atomic fluorescence spectrometry (AFS) [7], atomic absorption spectroscopy (AAS) [8], surface-enhanced Raman scattering (SERS) [9], inductively coupled plasma atomic emission spectrometry (ICP-AES) [10], Photo electrochemical spectrometry (ICP-MS) [11], and on-line coupled systems (gas chromatography or liquid chromatography coupled with AAS, AFS, or ICP-MS [12,13], selective cold vapor atomic fluorescence spectrometry [14] and selective Voltammetric [15,16] have been used for Hg^{2+} determination.

Despite the selectivity and specificity of some analytical techniques, they are too expensive, complex, cumbersome, and time-consuming and requires a larger amount of samples. On the other.

Hand, electrochemical techniques have many benefits in comparison to the others, for example, simplicity, low-cost, accurateness, sensitivity, ability to the determination. Voltammetric methods such as anodic stripping voltammetry (ASV) are one of the best and powerful

electrochemical methods for determination of the nano molar concentration of heavy metal ions, because of preconcentration step [17].

In the last decade, some electrochemical sensors have been developed using several kinds of functional materials to improve selectivity, stability and the sensor response. The electrochemical sensors have been modified by functional materials. Theses material included various nano-materials such as metal nanoparticles (NPs), metal oxide NPs, polymeric NPs, carbon-based nanomaterials and quantum dots [18-20]. A wide variety of nanocomposites have been recently applied to fabricate the modified sensors because of their biological compatibility, high-specific surface area, chemical stability, excellent catalytic activity and conductivity [21,22]. These nanocomposites including metal oxide NPs and multi metal oxide nanocomposites have been utilized as catalysts owing to their unique electronic structure. Hence, the synthesis of metal oxide nanocomposites has been investigated in order to evaluate their performance in different applications such as fuel cells, super capacitors, and electrochemical Sensors [23].

The electrochemical detection of Hg^{2+} ion in presence of other ions that can make interference in the detection step is a challenge in the voltammetric method. However the overlap of corresponding peaks is a major problem of simultaneous determination of heavy metal ions, there is an increasing interest at development of carbon paste electrode (CPE) and modified CPE as working electrode for separation of peaks [24]. To improve the selective interaction between analyses and sensing layer, chemically modified matrices have been used. The applied matrices was enhanced the conductivity, surface area and sensitivity of modified electrode [25].

The other advantages of CPEs is easy of fabrication, have a low cost flexible substrate for modification, low ohmic resistance, high sensitivity, chemical inertness, renewable surface and compatibility with different kind of modifiers. The sensing properties of modified CPEs are widely depend on the nature of used materials in sensing layer. In recent years, the synthesis of nanoparticles has opened new horizons in designing of advanced electrochemical systems [26].

The synergetic effects of composite nanomaterials can differentiate their catalytic performance from each one of the components. The composition and morphology of metal oxide NPs are controllable, and the lattice matching between metal oxides can be easily realized. Thus, metal oxides are suitable for support matrices. Several kinds of nanocomposites have been synthesized with two or three different metal oxide NPs, which have high specific surface area and catalytic activity [27]. Recently, the novel properties of multi metal oxides nanocomposites have been considered which are suitable for microelectronic devices, catalyst and semiconductor devices [28]. There are many types of research carried out for the synthesis of bimetal-oxide nanocomposites such as $\text{Co}_3\text{O}_4\text{-CeO}_2$ [29], CeO-ZnO , $\text{Co}_3\text{O}_4\text{-ZnO}$, and ternary metal oxide nanocomposites such as $\text{Co}_3\text{O}_4\text{-CeO}_2\text{-ZnO}$ nanocomposite [30].

In the present study, a green method has been developed for synthesis of $\text{Co}_3\text{O}_4\text{-CeO}_2\text{-ZnO}$ nanocomposite and applied for preparing of modified CPE to improve the sensitivity and selectivity. Final products were characterized by some common methods including Transmission Electron microscopic (TEM), X-ray powder diffraction (XRD), and Fourier transform infrared (FT-IR). Under optimum

condition, the $\text{Co}_3\text{O}_4\text{-CeO}_2\text{-ZnO/CPE}$ showed high activity to electro-oxidation of Hg^{2+} ion. The $\text{Co}_3\text{O}_4\text{-CeO}_2\text{-ZnO/CPE}$ was used for individual and simultaneous determination of trace amounts of Hg^{2+} ion in different as a real sample.

2. EXPERIMENTAL

2.1. Reagents and materials

All reagents were of analytical grade and used as received without any further purification. Laboratory glassware were kept overnight in a 10% (v/v) HNO_3 solution and then rinsed with DDW. Graphite powder (10 μm average particle size) and pure paraffin oil were purchased from Merck. $\text{Co}(\text{NO}_3)_2 \cdot 6\text{H}_2\text{O}$, were purchased from Merck company and used in order to synthesis $\text{Co}_3\text{O}_4\text{-CeO}_2\text{-ZnO}$ nanocomposite. Stock solutions of Hg^{2+} (1000 mg L^{-1}) were prepared by dissolving appropriate amounts of HgCl_2 (Merck) in DDW, respectively. More diluted solutions were prepared daily using this stock solution. Buffer solutions were prepared from 1 ml of citrate/acetate/phosphate (1.0 M), phosphate (1.0 M) buffers (pH 2–7) were prepared and they were tested as supporting.

2.2. Instrumentation

The electrochemical cell was assembled with a conventional three-electrode system. A platinum wire, an Ag/AgCl/KCl (3 mol L^{-1}) electrode, modified or unmodified CPEs were employed as an auxiliary electrode, a reference electrode and working electrodes, respectively. The prepared nanocomposite was characterized by Transmission Electron Microscopy (TEM) images (Zeiss EM902A), XRD (38066 Riva, d/G. Via M. Misiones, 11/D (TN)). The structure and phase evaluation of prepared samples was carried out by using Philips Xpert MPD, X-ray diffractometer with $\text{CuK}\alpha$ radiation at beam acceleration conditions of 40 kV/35 mA.

The pH/Ion meter (model-728, Metrohm Company, Switzerland, Swiss) was used for the pH measurements.

2.3. Samples preparation

Different standard amounts of Hg^{2+} were spiked into 100 ml samples of Ramin power plant cooling water, Maroon dam water, Dez dam water, Karon River water, Ahvaz drinking water and hospital Ahvaz water samples were collected in acid-leached polyethylene bottles. All water samples were collected from (Ahvaz, Iran). Filtered through 0.45 μm Millipore cellulose acetate membrane filters to remove particles and diluted with distilled water to the ratio of 1:1. The samples were then adjusted to $\text{pH}=5.5$ and immediately analyzed [31].

2.4. Preparation of $\text{Co}_3\text{O}_4\text{-CeO}_2\text{-ZnO}$ nanocomposite and Co, CeO_2 and ZnO nanoparticles.

The $\text{Co}_3\text{O}_4\text{-CeO}_2\text{-ZnO}$ tri-metallic nanocomposite was synthesized by co-precipitation procedure. In the first step, the solution of $\text{Co}(\text{NO}_3)_2 \cdot 6\text{H}_2\text{O}$ and $\text{Zn}(\text{NO}_3)_2 \cdot 6\text{H}_2\text{O}$ (each of the solution was 0.25 M) were mixed in a 1:1 molar ratio and stirred for 2 h at room temperature. In the next step, the solutions of (1 M) by same molar ratio were added to the previous solution. The solution was stirred for 3 h at room temperature.

Finally, the precipitate was separated by centrifuge and washed by DDW. The obtained precipitate was dried in an oven at 90 $^\circ\text{C}$ for 1 h and at 200 $^\circ\text{C}$ for 3 h, respectively. To achieve the $\text{Co}_3\text{O}_4\text{-CeO}_2\text{-ZnO}$ tri-metallic nanocomposite, the dried precipitate was sintered in a furnace at 450 $^\circ\text{C}$ for 5 h. In this stage, the nanocomposite was annealed at 950 $^\circ\text{C}$ for 10 h to convert carbonate to oxide sample. The Co and ZnO nanoparticles were also synthesized by the same method without addition of other ions [30].

2.5. Sensor preparation

The bare CPE was prepared by hand-mixing of a pure graphite powder and a certain amount of paraffin oil (ratio of 70:30 w/w) in an agate mortar. To prepare the $\text{Co}_3\text{O}_4\text{-CeO}_2\text{-ZnO/CPE}$ modified electrode, a 10% w/w portion of $\text{Co}_3\text{O}_4\text{-CeO}_2\text{-ZnO}$ was mixed with 60% w/w graphite powder. It was dispersed in dichloromethane to well-mixing of the composite and was stirred until dichloromethane evaporated completely [29,30].

Then the paraffin oil (30 % w/w) was added and mixed until the uniform paste was obtained. This paste preparation method was applied to provide a reproducible sensor after each surface polishing of the electrode. All amount of each paste was transferred into an insulin syringe and packed carefully to avoid possible air gaps and improve the electrode resistance. A copper wire (1.0 mm diameter) was inserted into the unmodified and modified electrode to establish the electrical contact.

2.6. Analytical procedure

Square wave anodic stripping voltammetry (SWASV) technique was used for determination of analyses under optimized condition. It was performed in a 20 mL electrochemical cell containing acetic acid/tri chloric acetate buffer as a supporting electrolyte medium. Hg^{2+} ion was deposited at the reduction potential of $-0.8 \text{ V vs. Ag/AgCl}$ for 120 s. Re-Oxidation of Hg^0 to Hg^{2+} were performed in anodic stripping step in the potential range of -0.8 to $0.2 \text{ V vs. Ag/AgCl}$. Before any measurement, in pre-conditioning step, a potential of $1.0 \text{ V vs. Ag/AgCl}$ for 60 s was performed to ensure dissolution of the remaining deposits on the surface of $\text{Co}_3\text{O}_4\text{-CeO}_2\text{-ZnO/CPE}$. The pre-concentration and cleaning steps were done while the solution of the

electrochemical cell was stirred. The peak current potential -0.4 V vs. Ag/AgCl for Hg^{2+} ion, was obtained.

3. RESULTS AND DISCUSSION

3.1. Characterization of synthesized nanocomposite.

The morphology, structure, and size of synthesized materials were investigated by SEM and TEM. The SEM and TEM image of $\text{Co}_3\text{O}_4\text{-CeO}_2\text{-ZnO}$ are shown in Fig. 1a and Fig. 1b, respectively. It is found that $\text{Co}_3\text{O}_4\text{-CeO}_2\text{-ZnO}$ tri-metallic nanocomposite with the average size of about 17 nm (nanoparticles with diameters in the range of 8–25 nm) was synthesized by the co-precipitation procedure. It is

noticeable that the synthesized method is efficient to prevent the aggregation of Co_3O_4 , CeO_2 , and ZnO nanoparticles.

Hence, the synthesized nanocomposite has a high specific surface area. To confirm the chemical structure of the synthesized nanocomposite, the FT-IR spectra of the $\text{Co}_3\text{O}_4\text{-CeO}_2\text{-ZnO}$ tri-metallic nanocomposite (Fig. 1c) was recorded. The FT-IR spectrum of the nanocomposite illustrates the absorption band at about 3500, 1400, 1100, 1000, 820, 615 and 460 cm^{-1} which confirm the presence of O-H of the carboxylic groups, CO_3^{2-} , C-O, O-H, Ce-O, Zn-OH, and Zn-O. This absorption bands indicate the effectively synthesis of $\text{Co}_3\text{O}_4\text{-CeO}_2\text{-ZnO}$

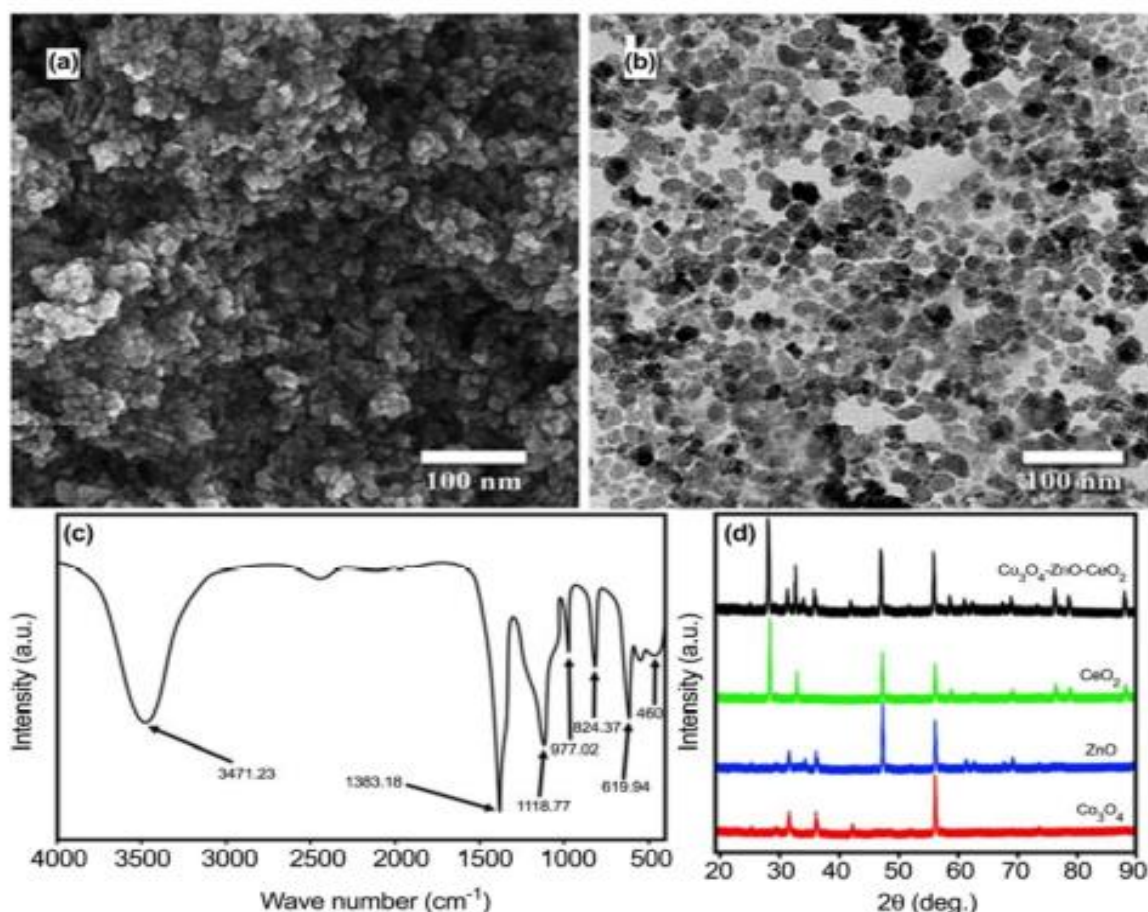


Fig. 1. (a) SEM, (b) TEM, (c) FT-IR spectra of $\text{Co}_3\text{O}_4\text{-CeO}_2\text{-ZnO}$ nanocomposite tri-metallic nanocomposite, and (d) XRD patterns of Co_3O_4 , CaO_2 , ZnO and $\text{Co}_3\text{O}_4\text{-CeO}_2\text{-ZnO}$ nanocomposite.

multi-metallic nanocomposite [32]. The XRD patterns of $\text{Co}_3\text{O}_4\text{-CeO}_2\text{-ZnO}$ nanocomposite, $\text{Co}_3\text{O}_4\text{-CeO}_2$ and ZnO nanoparticles are shown in Fig. 1d. The XRD pattern of Co shows three peaks about $2\theta = 31.77^\circ$, 36.28° and 56.42° which matches well with the standard sample. The XRD pattern of the Co nanoparticles illustrate some peaks about $2\theta = 28.5^\circ$, 33.09° , 47.46° , 56.42° , 59.10° , 69.37° , 79.13° , 76.79° and 88.55° which is matched with the standard sample. The XRD pattern of ZnO nanoparticles represents seven peaks about $2\theta = 31.77^\circ$, 34.27° , 36.26° , 47.46° , 56.42° , 62.99° and 69.10° , which are adjusted with the standard sample. According to the obtained results of XRD pattern of $\text{Co}_3\text{O}_4\text{-CeO}_2\text{-ZnO}$ nanocomposite tri-metallic nanocomposite, the positions of diffraction peaks are in agreement with the standard samples of $\text{Co}_3\text{O}_4\text{-CeO}_2\text{-ZnO}$ nanocomposite [33].

3.2. Voltammetric behavior of Hg^{2+} on the surface of unmodified and modified electrodes

To explain the function of modifiers in the electrodes preparing process, the stripping voltammograms were recorded with different electrodes. Square-wave

voltammograms of a solution containing 10.0 nM Hg^{2+} in phosphate buffer (pH = 5.5, 0.1M) at the bare CPE and $\text{Co}_3\text{O}_4\text{-CeO}_2\text{-ZnO/CPE}$ by accumulation potential -0.4 V for 120 s in the potential range -0.8 to 0.2 V vs. Ag/AgCl are shown in Fig. 2.

Voltammograms of the solution at bare CPE exhibited no stripping peaks in used condition. After Modifying the sensing layer of electrode with $\text{Co}_3\text{O}_4\text{-CeO}_2\text{-ZnO}$ nanocomposite, the Co ZnO/CPE Did not show any oxidation peak in the absence of the analytcs. After adding each analyte, two distinct stripping peaks can be seen for Hg^{2+} ion, the peak separation of 7.5 V vs. Ag/Ag/Cl. This peak was attributed to facilitating electron transfer between Hg^{2+} ion and $\text{Co}_3\text{O}_4\text{-CeO}_2\text{-ZnO/CPE}$. It is also owing to increasing of the surface area of the electrode. Based on these observations, the Co ZnO/CPE can be useful for determination of Hg^{2+} ion in aqueous solution [34]. The response of modified electrode is dependent on many factors including pH of solution, accommodation potential, time, and the instrumental parameters of SWV. These parameters were optimized to achieve the best peak shape, maximum current, and the lowest detection limit.

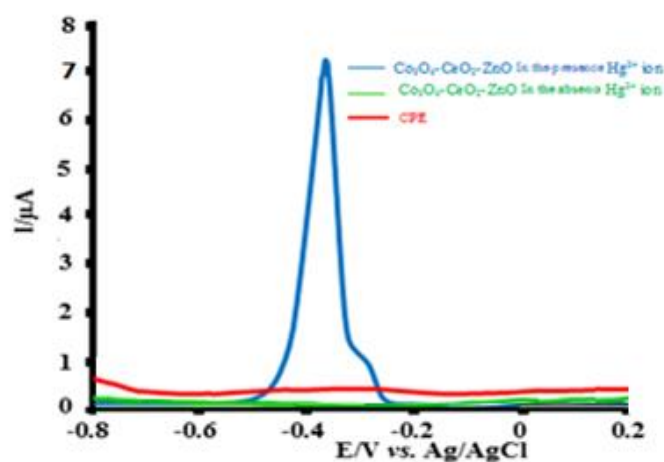


Fig. 2. SW voltammograms in the absence and present 10.0 nM of Hg^{2+} , on the surface of bare CPE, and $\text{Co}_3\text{O}_4\text{-CeO}_2\text{-ZnO/CPE}$.

3.3. Effect of pH on the response of modified electrode

The effect of pH on the current responses (10.0 nM of Hg^{2+} ions) on the $\text{Co}_3\text{O}_4\text{-CeO}_2\text{-ZnO/CPE}$ was investigated in the range of 2.0 to 7.0 by SWV. The results are shown in (Fig. 3a). The stripping currents for the both analytes have been raised by increasing of pH up to 5.5 and the maximum oxidation peak current appeared at pH 5.5. The peak current was decreased by further increasing of pH; it may be owing to the Hg^{2+} ions hydrolysis. Hence, the pH of 5.5 was selected for subsequent experiment [34,35].

In order to choose the optimal buffer, three buffers (citrate, acetate and phosphate buffer) were investigated that acetate buffer was the best (Fig. 3b). Furthermore, 1.0 mL of phosphate buffer was selected as optimum (Fig. 3b).

3.4. Effect of deposition potential, deposition time and instrumental parameters on the voltammetric currents

Sensitivity and detection limit depend on deposition potential, accumulation time and instrumental parameters hence optimization of these parameters is necessary.

The effect of deposition potential on the stripping response of 10.0 nM Hg^{2+} ion were studied while the deposition potential was changed from -1.3 and -0.9 V vs.

Ag/AgCl on $\text{Co}_3\text{O}_4\text{-CeO}_2\text{-ZnO/CPE}$ under optimum conditions (Fig. 4a). The study represents that the electrode response increase gradually by changing the deposition potential up to -1.1V vs. Ag/AgCl and accumulation time up to 120 s. On the other hand, the stripping responses for Hg^{2+} ion have decreased while the deposition potential was more negative than -1.1V vs. Ag/AgCl , because of the reduction of other chemicals at these potentials. The hydrogen evolution was also started at such negative potentials. The background current was more than the other potential range. Hence, the potential of -1.1V vs. Ag/AgCl was selected as an optimum deposition potential [36].

The effect of deposition time on the stripping responses of Hg^{2+} ions was studied from 30 to 210 s with a deposition potential of -1.1V , and it has been found that the oxidation response is increased by increasing of accumulation time up to 120 s (Fig. 4b). This is owing to the fact that the longer collection time caused more Hg ions to get accumulated at the electrode/solution interface onto modified surface, hence current increases. It can be seen that after 120 s, the stripping currents becomes approximately constant owing to surface saturation [37]. Hence, the accumulation time of 120 s was selected and used as an optimum condition.

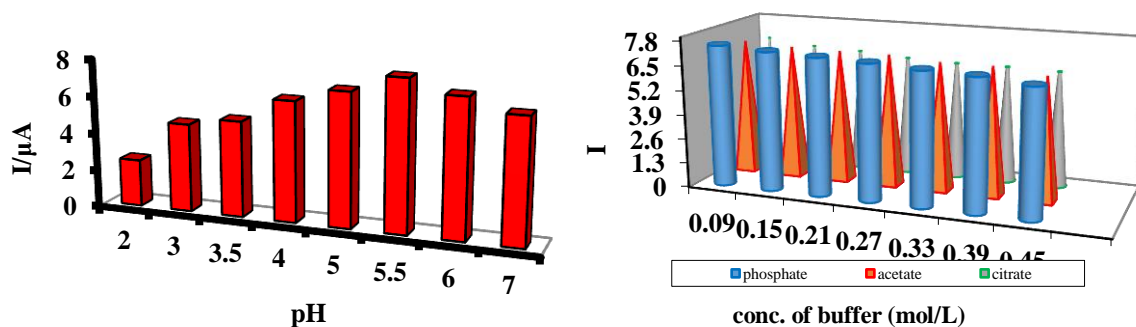


Fig. 3. (a) Effect of pH on the on the voltammetric currents for 10.0 nM of Hg^{2+} ions solution. (b) Effect of buffer on the surface plasmon intensity (: aqueous sample volume, 10 mL; $[\text{Hg}^{2+}$ ions] = 10.0 nM, pH = 5.5).

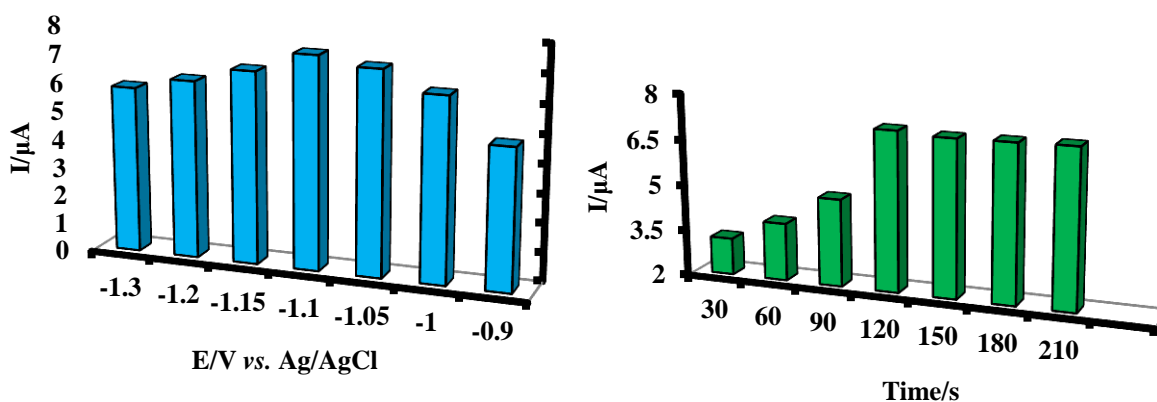


Fig. 4. (a) Effect of deposition potential on the voltammetric currents for 10.0 nM Hg^{2+} solution in pH = 5.5. (b) Effect of deposition time on the voltammetric currents for 10.0 nM Hg^{2+} solution in pH = 5.5.

3.5. Measurement of Hg^{2+} ion in standard solutions and calibration curve.

Analytical performance of $\text{Co}_3\text{O}_4\text{-CeO}_2\text{-ZnO/CPE}$ for determination of Hg^{2+} ion. Under the optimum condition, SWV were recorded for different concentration of Hg^{2+} ion on the $\text{Co}_3\text{O}_4\text{-CeO}_2\text{-ZnO/CPE}$. When concentrations of the both analyses were simultaneously increased, two separated stripping peaks with two linear range of 0.03–35.0 nM for Hg^{2+} ion were obtained respectively [38]. The linear regression equations of Hg^{2+} ion and coefficients of determination was $I_{pa} = 0.4988C_{\text{Hg}} + 0.319$ ($R=0.9986$), respectively (Fig. 5a and 5b). LOD of the modified $\text{Co}_3\text{O}_4\text{-CeO}_2\text{-ZnO}$ nanocomposite and Hg^{2+} ion electrode was calculated based on three times of standard deviation of the blank signals to calibration slope (3S/m). LODs were calculated 0.09 nM Hg^{2+} ion, respectively. For individual determination of each analyte, the concentration of Hg^{2+} ion was kept constant in 10.0 nM while concentration of Hg^{2+} ion was changed from 0.03 to 35.0 $\mu\text{g L}$ (Fig. 6) [39].

3.6. Evaluation of reproducibility and stability of the modified electrode

$\text{Co}_3\text{O}_4\text{-CeO}_2\text{-ZnO/CPE}$ electrode reproducibility by recording Square wave anodic stripping voltammetry (SWASV) (repeated) $n = 10$ (from constant concentrations of Hg^{2+} ion) 10.0 nM (at pH = 5.5 and extracting peak currents from each voltammogram studied The relative standard deviation (RSD) was calculated to be 2.3%, which indicates the excellent reproducibility of the modified electrode results and the high accuracy of the introduced analytical method. Also, the stability of the electrode by polishing the electrode surface and 10.0 nM of Hg^{2+} ion voltammogram was recorded at pH = 5.5 and then the electrode was stored for two weeks in ambient conditions and the voltammogram was recorded and compared with the initial voltammogram [40,41]. It was found that the peak currents were equal after two weeks. 96% were their initial values. This test was performed on the electrode again after one month and three months and the obtained currents had reached 95.2% and 95.6% of their initial

values, respectively, which indicates the good stability of the electrode and the possibility. It has a long shelf life. The stability of the proposed electrochemical sensor was investigated by detecting the SWASV responses of the electrode. The response of electrode for 10.0 nM of Hg^{2+} $\text{Co}_3\text{O}_4\text{-CeO}_2\text{-ZnO}$ nanocomposite retained 95.6% of its initial stripping response after a period of 21 days. The results indicate that the $\text{Co}_3\text{O}_4\text{-CeO}_2\text{-ZnO/CPE}$ has excellent repeatability, reproducibility, and long-term stability.

3.7. Optimum values of parameters

The optimum values of parameters are demonstrated in Table.1. The method can be used as an alternative method for Hg^{2+} ion measurement owing to advantages like excellent selectivity and sensitivity, low cost, simplicity, low detection limit and no

need in utilizing organic harmful solvent.

3.8. Interference Studies

The electro active compounds that are present in the real samples might be a potential interference during the electrochemical determination of the analytes. Among what we studied were also the interaction between anions and cations on Hg^{2+} ion direction. To perform these studies, various ions were introduced into the solution that contained 100 ng mL of Hg^{2+} ion and then applying the general procedure [7, 15, 42].

As exhibited in (Table.2), the tolerance limit was determined as the max concentration of the interfering substance which resulted in an error less than ($\pm 5\%$) for determination of Hg^{2+} ion. So selectivity of the recommended method was proven.

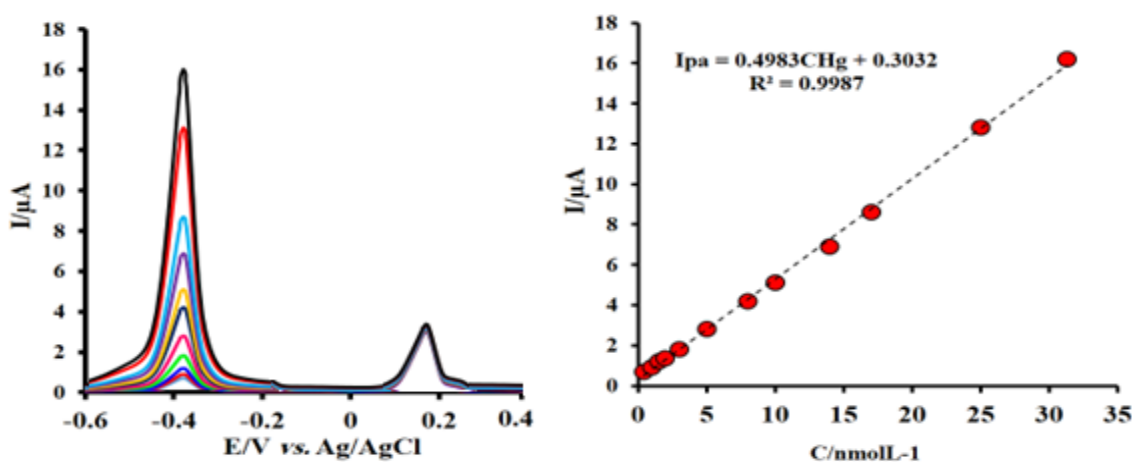


Fig. 5. (a) SW voltammograms using C_{Hg} the analytes concentrations. $\text{Co}_3\text{O}_4\text{-CeO}_2\text{-ZnO/CPE}$ for Hg^{2+} ion (0.03–35.0 nM) under optimum condition (b) Calibration plot of the voltammetric currents as a function of the analytes concentrations.

Table 1. Investigation of method repeatability at conditions

Parameter	Optimum Value for Hg^{2+} ion
Hg^{2+} ion	(10.0 nM)
pH	5.5
Equilibration time (s)	(120 s)
Linear range (LDR)	(0.03 –35.0 μgL^{-1})
Detection limit (LOD)	(0.09 nM)
Relative Standard Deviations (RSD)	(2.3%)
Advantages	High repeatability, sensitivity, selectivity, wide linear range a

Table 2. Limit of tolerance foreign ions on determination of Hg²⁺ ion (n=6)

Foreign species	Tolerance limit (ng mL ⁻¹)
NH ₄ ⁺ , Mg ²⁺ , Na ⁺ , K ⁺ , Ca ²⁺	1000
CO ₃ ²⁻ , SO ₄ ²⁻ , Cl ⁻ , I ⁻	1000
Cr ³⁺	250
Ag ⁺ , Fe ²⁺ , Fe ³⁺	100

3.9. Analysis of spices sample

Several tests were carried out in order to determination of Hg²⁺ ion in different real samples. As it can be seen in Table 3, the results of the measurements are comprised to those obtained by Square wave anodic stripping voltammetry (SWASV) method which confirmed the accuracy and reliability of the method [43,44]. Hence the proposed method can be used for individual and simultaneous detection of Hg²⁺ ion in different real samples. The results showed that the obtained data of proposed method are in good agreement with the reference method. Linear range and detection limit of the presented method was comprised with some recently reported methods (Table. 3).

3.10. Comparison of this method with other methods

A comparison of the proposed method with the other previously reported methods demonstrates the feasibility of SWASV method and its reliability for the analysis of Hg²⁺ ions (Table 5). The LOD and LDR in this work are comparable with and lower than some studies. RSD is better than some and comparable with those of the other studies. It can be concluded that SWASV is a sensitive method that can be used for the pre-concentration and extraction of Hg²⁺ ions from environmental samples.

4. CONCLUSIONS

This study provides a new modified carbon

paste electrode based on Co₃O₄-CeO₂-ZnO tri-metallic nanocomposite for determination of Hg²⁺ ion in Ramin power plant cooling water, Maroon dam water, Dez dam water, Karon River water, Ahvaz drinking water and hospital Ahvaz water. The obtained results suggest that Co₃O₄-CeO₂-ZnO nanocomposite is better than some other modifier of CPE for the electrochemical determination of Hg²⁺ ion. The calibration curve was linear in the range of (0.03-35.0 nM). The standard deviation of less than (3%), and detection limits (3S/m) of the method (0.09 nM) for Hg²⁺ ion were obtained for the proposed electrochemical sensor by Co₃O₄-CeO₂-ZnO/CPE, respectively. Hence, the proposed modified electrode can be used long term, providing a low detection limit (sub-nano molar), high selectivity, reproducibility, repeatability for determination of both analytes. The electrochemical sensor could also be renewed quickly and easily by mechanical polishing with a filter paper whenever needed. Consequently, the results showed the studied method would be a promising method to use in routine analytical applications.

ACKNOWLEDGEMENT

The authors gratefully acknowledge partial support of this work by the Islamic Azad University, Branch of Omidyeh, Iran.

Table 3. Analytical results of the determination of Hg²⁺ ion content and recovery test of Hg²⁺ ion in water samples with the proposed method (n=5)

Samples	Added ($\mu\text{g mL}^{-1}$)	Founded ($\mu\text{g mL}^{-1}$)	RSD %	Recovery %
Hospital Ahvaz	0.00	0.30	2.6	----
River water	10.0	0.54	1.5	98.9
Ramin power plant	0.00	0.32	3.6	----
cooling water	10.0	0.54	2.3	101.6
Karon River	0.00	0.93	1.1	----
warerAhvaz	10.0	1.44	0.9	103.4
Dez dam water	0.00	0.83	3.9	----
	10.0	1.35	2.3	104.0
Maroon dam water	0.00	0.49	2.9	----
	10.0	0.74	1.8	102.0

Table 4. Comparisons of proposed method with other grapheme – based Hg²⁺ ion sensor

Sensing platform / Method	LOD (nM)	Working Range (LDR)	Detection time	Ref
SsDNA-NanoAu-G - SWV	0.001 aM	1.0 aM-100 nM	60 min	[25]
AuNPs/G - SWASV	30 pM	10-300 nM	21 min	[26]
PPy-3D rGO - SWASV	30 nM	0.1-110 nM	20 min	[28]
NiS-rGO - SWASV	8 nM	0.1-110 nM	20 min	[29]
3D Au/G – SWV	50 aM	0.1 fM-0.1 μM	180 min	[34]
Hydroxyapatite (HA) nanoparticles modified GCE SWA	141 nM	0.2-210 μM	240 sec	[45]
(CBNP-AuNP-SPE) SWASV	3 nM	0.01 -50 μM	10 min	[46]
Nafion/cys-Au@Ag BMNps/GCE DPV	10 nM	0.1 -100 μM	300 sec	[47]
Co ₃ O ₄ -CeO ₂ -ZnO - SWASV	10 nM	0.03-35.0 nM	120 sec	This work

^aLDR, linear dynamic range is the minimum detectable concentration and the largest concentration that the response factor @ falls outside.

REFERENCES

- [1] L.R.P. Mandoc, I. Moldoveanu, R.I. Stefan-van Staden, E.M. Ungureanu, *Microsystem Technologies*. 23 (2017) 1141.
- [2] S. Sobhanardakani, R. Zandipak, *J. Clean. Techn. Environ. Policy*. 19 (2017) 1913.
- [3] Y. Zhang, L. Zhang, B. Han, P. Gao, Q. Wu, A. Zhang, *Sensors & Actuators: B. Chemical*. 272 (2018) 331.
- [4] X. Guo, B. Du, Q. Wei, J. Yang, L. Hu, L. Yan, W. Xu, *J. Hazar. Meter*. 278 (2014) 211.
- [5] P.J. Mafa, A.O. Idris, N. Mabuba, O.A. Arotiba, *Talanta*. 153 (2016) 99.
- [6] B. Babamiri, A. Salimi, R. Hallaj, *Biosens. Bioelectron*. 102 (2018) 328.
- [7] S. Prabu, S. Mohamad, *J. Mol. Structure* 44 (2020) 65.
- [8] N. Bansal, J. Vaughan, A. Boullemant, *Microchem. J.* 113 (2014) 36.
- [9] Y. Tian, H.F. Wang, L.Q. Yan, X.F. Zhang, A. Falak, P.P. Chen, F.L. Dong, L.F. Sun, W.G. Chu, *Chinese Physics. B*. 27 (2018) 77406.
- [10] G. Jarzynska, J. Falandysz, *J. Environ. Sci. Health A*. 46 (2011) 569.
- [11] G. Wen, X. Wen, M.M.F. Choi, S. Shuang, *Sensors and Actuators B-Chemical*. 221 (2015) 1449.
- [12] X. Chen, C. Han, H. Cheng, *J. Chromatogr. A* 1314 (2013) 86.
- [13] S.S. de Souza, A.D. Campiglia, F. Barbosa Jr, *Analytica Chimica Acta*. 761 (2013) 11.
- [14] S. Abbasi, A. Bahiraei, F. Abbasai, *Food chem*. 129 (2011) 1274.

- [15] Q. Zhao, Y. Chai, R. Yuan, J. Luo, *Sens. Actuators B-Chem.* 178 (2013) 379.
- [16] N. Zhou, H. Chen, J. Li, L. Chen, *Microchimica Acta.* 180 (2013) 493.
- [17] S. Davoudi, M.H. Givianrad, M. Saber-Tehrani, P. Aberoomand Azar, *Russian J. Electrochemistry.* 56 (2020) 506.
- [18] P. Borthakur, G. Darabdhara, M.R. Das, R. Boukherroub, S. Szunerits, *Sensors and Actuators Chemical. B.* 244 (2017) 684.
- [19] H. Xie, Y. Niu, Y. Deng, H. Cheng, C. Ruan, G. Li, W. Sun, *J. Chin. Chem. Soc.* 61 (2020) 1.
- [20] H. Zeinali, H. Bagheri, Z. Monsef-Khoshhesab, *Mater. Sci. Eng. C.* 71 (2017) 356.
- [21] N. Zhou, J. Li, H. Chen, C. Liao, L. Chen, *Analyst.* 138 (2013) 1091.
- [22] F. Marahel, L. Niknam, E. Pournamdari, A. Geramizadegan, *J. Iran. Chem. Soc.* 19 (2022) 3377.
- [23] W. Chansuvarn, T. Tuntulani, A. Imyim, *Trends Anal. Chem.* 65 (2015) 83.
- [24] H. Bagheri, A. Afkhami, H. Khoshsafari, *Anal. Chim. Acta.* 870 (2015) 56.
- [25] F. Marahel, *Int. J. Environ. Anal. Chem.* 101 (2021) 1.
- [26] J. Gong, T. Zhou, D. Song and L. Zhang, *Sens. Actuators. B.* 150 (2010) 491.
- [27] J. Kaur, S. Bhukal, K. Gupta, M. Tripathy, S. Bansal, S. Singhal, *J. Mater. Chem. Phys.* 177 (2016) 512.
- [28] M. Wang, W. Yuan, X. Yu and G. Shi, *Anal. Bioanal. Chem.* 406 (2014) 6953.
- [29] T.D. Vu, P.K. Duy, H.T. Bui, S.H. Han, H. Chung, *Sensors and Actuators Chemical, B.* 281 (2019) 320.
- [30] F. Marahel, L. Niknam, *J. Environ. Sci. Health B.* 57 (2022) 489.
- [31] H. Shafiekhani, F. Nezam, Sh. Bahar, *J. Serb. Chem. Soc.* 82 (2017) 317.
- [32] S. Davoudi, M.R. Asghari, *J. Appl. Chem. Res.* 16 (2022) 57.
- [33] S. Cinti, F. Santella, D. Moscone, F. Arduini, *Environ. Sci. Pollut. Res.* 23 (2016) 8192.
- [34] P. Mahato, S. Saha, E. Suresh, R. Di Liddo, P.P. Parnigotto, M.T. Conconi, M.K. Kesharwani, B. Ganguly, A. Das, *Inorg. Chem.* 51 (2012) 1769.
- [35] L. Shi, Y. Wang, S. Ding, Z. Chu, Y. Yin, D. Jiang, J. Luo and W. Jin, *Biosens. Bioelectron.* 89 (2017) 871.
- [36] M.B. Gumpu, M. Veerapandian, U.M. Krishnan, J.B.B. Rayappan, *Talanta.* 162 (2017) 574.
- [37] H. Park, S.-J. Hwang and K. Kim, *Electrochem. Commun.* 24 (2012) 100.
- [38] Y. Yang, M. Kang, S. Fang, M. Wang, L. He, J. Zhao, H. Zhang and Z. Zhang, *Sens. Actuators. B.* 214 (2015) 63.
- [39] S.L. Pan, K. Li, L.L. Li, M.Y. Li, L. Shi, Y.H. Liu, X.Q. Yu, *Chem. Commun.* 54 (2018) 4955.
- [40] A. Afkhami, H. Bagheri, H. Khoshsafari, M. Saber-Tehrani, M. Tabatabaee, A. Shirzadmehr, *Anal. Chim. Acta.* 746 (2012) 98.
- [41] S.S. Hassan Sirajuddin, A.R. Solangi, T.G. Kazi, M.S. Kalhor, Y. Junejo, Z.A. Tagar, N.H. Kalwar, *J. Electroanal. Chem.* 682 (2012) 77.
- [42] L. Cui, J. Wu, M.Q. Li, H.X. Ju, *Electrochem. Commun.* 59 (2015) 77.
- [43] Z. Wu, L. Jiang, C. Xu, Y. Ye, X. Wang, *J. Solid State Electrochem.* 16 (2012) 3171.
- [44] A.C. Lokhande, N.M. Shinde, A. Shelke, P.T. Babar, J.H. Kim, *J. Solid State Electrochem.* 21 (2017) 2747.
- [45] L. Laffont, T. Hezard, P. Gros, L.E. Heimbürger, J.E. Sonke, P. Behra, D. Evrard, *Talanta.* 141 (2015) 26.
- [46] F. Cai, Q. Zhu, K. Zhao, A. Deng, J. Li, *Environ. Sci. Technol.* 49 (2015) 5013.
- [47] S. Siddiqui, A. Nafady, H. M. El-Sagher, S. I. Al-Saeedi, A. M. Alsalmeh, F. N. Talpur, S. T.H. Sherazi, M. S. Kalhor, M. R. Shah, S. T. Shaikh, M. Arain, S. K. Bhargava, *J. Solid State Electrochemistry.* 23 (2019) 2073.

الکتروآنالیز مقدار ردیابی یون جیوه در نمونه‌های آب با استفاده از سنسور $\text{Co}_3\text{O}_4\text{-CeO}_2\text{-ZnO/CPE}$
و روش ولتامتری سلب آندی موج مربعی (SWASV)

شهناز داوودی*

دانشگاه آزاد اسلامی، واحد امیدیه، گروه شیمی، واحد امیدیه، ایران

چکیده

این مطالعه ساخت یک حسگر الکتروشیمیایی جدید را توصیف می‌کند و برای تعیین یون جیوه کاربرد دارد. این حسگر با استفاده از یک پایه نانوکامپوزیت جدید بر روی $\text{Co}_3\text{O}_4\text{-CeO}_2\text{-ZnO/CPE}$ تهیه شد. اگرچه روش‌های دیگر (کروماتوگرافی گازی یا مایع، الکتروفورز، تزریق جریان) برای اندازه‌گیری یون جیوه دارای مزایایی مانند دقت و تکرارپذیری عالی است، اما محدودیت‌هایی مانند اندازه‌گیری طولانی مدت، هزینه بالای تجهیزات دارد. در این مطالعه برای تعیین یون جیوه از حسگر $\text{Co}_3\text{O}_4\text{-CeO}_2\text{-ZnO/CPE}$ و روش ولتامتری استفاده شد. منحنی کالیبراسیون خطی در محدوده $0/03$ تا $35/0$ میکروگرم در لیتر) بود. انحراف استاندارد کمتر از $(/3)$ و محدودیت‌های تشخیص (S/m^3) روش $(0/09)$ نانومولار) برای یون جیوه برای سنسور الکتروشیمیایی پیشنهادی توسط $\text{Co}_3\text{O}_4\text{-CeO}_2\text{-ZnO/CPE}$ با اطمینان $(/95)$ ارزیابی شد. در نهایت، $\text{Co}_3\text{O}_4\text{-CeO}_2\text{-ZnO/CPE}$ به عنوان یک سنسور الکتروشیمیایی با موفقیت برای تعیین یون جیوه در نمونه‌های آب استفاده شده است.

کلید واژه‌ها: یون جیوه؛ الکتروود اصلاح شده؛ سنسور الکتروشیمیایی؛ روش ولتامتری

* مسئول مکاتبات: sdavoudi632@gmail.com